Estrogen Receptor Involvement in Noradrenergic Regulation of Ventromedial Hypothalamic Nucleus Glucoregulatory Neurotransmitter and Stimulus-Specific Glycogen Phosphorylase Enzyme Isoform Expression

A. S. M. H. Mahmood[1], Prabhat R. Napit[1], Md. Haider Ali[1], and Karen P. Briski[1] (ORCID)

Abstract

Norepinephrine (NE) directly regulates ventromedial hypothalamic nucleus (VMN) glucoregulatory neurons and also controls glycogen-derived fuel provision to those cells. VMN nitric oxide (NO) and γ-aminobutyric acid (GABA) neurons and astrocytes express estrogen receptor-alpha (ERα) and ER-beta (ERβ) proteins. Current research used selective ERα (1,3Bis(4-hydroxyphenyl)-4-methyl-5-[4-(2-piperidinylethoxy)phenol]-1H-pyrazole dihydrochloride) or ERβ (4-[2-phenyl-5,7-bis(trifluoromethyl)pyrazolo[1,5-a]pyrimidin-3-yl]phenol) antagonists to address the premise that these ERs govern basal and/or NE-associated patterns of VMN metabolic neuron signaling and astrocyte glycogen metabolism. Both ERs stimulate expression of the enzyme marker protein neuronal nitric oxide synthase, not glutamate decarboxylase$_{65/67}$. NE inhibition or augmentation of neuronal nitric oxide synthase and glutamate decarboxylase$_{65/67}$ profiles was ER-independent or -dependent, respectively. In both neuron types, VMN ERβ activity inhibited baseline alpha1- (α_1-) and/or alpha2- (α_2-)adrenergic receptor (AR) expression, but ERα and -β signaling was paradoxically crucial for noradrenergic upregulation of α_2-AR. NE inhibited glycogen synthase expression and exerted opposite effects on VMN adenosine monophosphate-sensitive glycogen phosphorylase (GP)-brain type (stimulatory) versus NE-sensitive GP muscle (inhibitory) via ERα or -β activity. Results document unique ERα and ERβ actions on metabolic transmitter and AR protein expression in VMN nitrergic versus GABAergic neurons. ER effects varied in the presence versus absence of NE, indicating that both neuron types are substrates for estradiol and noradrenergic regulatory interaction. NE-dependent ER control of VMN GP variant expression implies that these signals also act on astrocytes to direct physiological stimulus-specific control of glycogen metabolism, which may in turn influence GABA transmission.

The ventromedial hypothalamic nucleus (VMN) integrates nutrient and other cues to control glucostasis (Watts and Donovan, 2010; Donovan and Watts, 2014). VMN metabolic-sensory neurons adjust synaptic firing to supply a dynamic readout of neuroenergetic state (Oomura et al., 1969; Ashford et al., 1990; Silver and Erecińska, 1998). Characterized effector transmitters of

[1]School of Basic Pharmaceutical and Toxicological Sciences, College of Pharmacy, University of Louisiana Monroe

Corresponding Author:
Karen P. Briski, School of Pharmaceutical and Toxicological Sciences, College of Pharmacy, University of Louisiana Monroe, 356 Bienville Building, 1800 Bienville Drive, Monroe, LA 71201, United States.
Email: briski@ulm.edu

energy insufficiency within the broader mediobasal hypothalamus include nitric oxide (NO) and γ-aminobutyric acid (GABA), which correspondingly stimulate or suppress counter-regulatory hormone output (Chan et al., 2006; Fioramonti et al., 2010; Routh et al., 2014). Studies focusing solely on the VMN, excluding other mediobasal hypothalamus components, for example, arcuate and tuberal nuclei, show that the catecholamine neurotransmitter norepinephrine (NE) regulates expression of biosynthetic enzyme protein markers of local glucoregulatory signaling, for example, neuronal nitric oxide synthase (nNOS) and glutamate decarboxylase$_{65/67}$ (GAD$_{65/67}$; Ibrahim et al., 2019). Selective sampling of VMN NO and GABA neurons using laser-catapult microdissection indicates that these cells are likely to be direct substrates for noradrenergic regulation as these cells express alpha$_1$- (α_1-), alpha$_2$- (α_2-), and beta$_1$- (β_1-) adrenergic receptor (AR) proteins (Ibrahim et al., 2019; Uddin et al., 2019).

In female rats, the ovarian hormone estradiol regulates hypoglycemia-associated neuronal transcriptional activation in key hypothalamic metabolic loci (Nedungadi et al., 2006) and hypoglycemic hyperphagia, hyperglucagonemia, and hypercorticosteronemia (Briski and Nedungadi, 2009). The VMN is a target of estrogen control of glucose homeostasis as hormone delivery to that structure alters insulin-induced hypoglycemia in ovariectomized (OVX) female rats (Nedungadi and Briski, 2012). Intracerebroventricular effects of the estrogen receptor-alpha (ERα) antagonist 1,3-*Bis*(4-hydroxyphenyl)-4-methyl-5-[4-(2-piperidinylethoxy) phenol]-1*H*-pyrazole dihydrochloride (MPP) or ER-beta (ERβ) antagonist 4-[2-phenyl-5,7-*bis*(trifluoromethyl) pyrazolo[1,5-*a*]pyrimidin-3-yl]phenol (PHTPP) implicate these ERs in hypoglycemic suppression of VMN nNOS and augmentation of GAD$_{65/67}$ profiles in females (Mahmood et al., 2018). NO and GABA neurons are plausible substrates for estradiol action as both cell types express ERα, ERβ, and the transmembrane G protein-coupled estrogen receptor (GPER)/G protein-coupled receptor 30 proteins (Uddin et al., 2019). In the female rat, estradiol may modulate NO and/or GAD neuron receptivity to NE, as hypoglycemic patterns of AR protein expression are ER-dependent (Uddin et al., 2019). The present project used pharmacological tools alongside high-resolution microdissection/ high-sensitivity molecular analytical techniques to address the hypothesis that VMN ERα and/or ERβ modulate NE control of nitrergic and GABAergic neuron AR and signaling marker expression in the female rat. Current work employed a characterized hormone replacement paradigm in OVX rats that reestablishes physiological-like estradiol levels (Butcher et al., 1974; Goodman, 1978; Briski et al., 2001). After NE was administered to animals that were pretreated by intra-VMN delivery of MPP or PHTPP, the VMN was selectly harvested by the Palkovits micropunch dissection technique for Western blot for nNOS and GAD protein expression. In addition, VMN neurons were identified by immunocytochemical labeling as nNOS- or GAD$_{65/67}$-immunoreactive (-ir)- positive in advance of laser-catapult microdissection for nerve cell type-specific measurements of α_1-AR, α_2-AR, and β_1-AR protein expression.

Astrocytes store glycogen as an energy reserve, which is maintained by incorporation or liberation of glucose residues by opposing actions of glycogen synthase (GS) and glycogen phosphorylase (GP; Stobart and Anderson, 2013). Exogenous NE regulates VMN astrocyte GS and net GP protein content (Ibrahim et al., 2019) and affects VMN glucoregulatory signaling through control of astrocyte supply of the oxidizable glycolytic end product L-lactate (Mahmood et al., 2019). Multiple GP isoforms are expressed in the brain, including muscle- (GPmm) and brain (GPbb) types, which differ according to regulation by phosphorylation versus adenosine monophosphate (AMP; Nadeau et al., 2018). GPmm mediates noradrenergic augmentation of cortical astrocyte glycogenolysis *in vitro* (Müller et al., 2015), but NE effects on brain GPmm expression *in vivo* have not been investigated. Cell energy deficits amplify GPbb expression *in vitro* (Nadeau et al., 2018). We observed that exogenous NE upregulates VMN GPbb and GAD$_{65/67}$ and that these responses are abolished by lactate transport blockade (Mahmood et al., 2019). Our studies also show that hindbrain A2 noradrenergic lactoprivic signaling exerts opposite effects on VMN GPbb versus GPmm profiles *in vivo* (Briski and Mandal, 2019). Although female rat VMN astrocytes are directly sensitive to estradiol by virtue of ER expression (Mahmood et al., 2018, 2019), involvement of these ERs in noradrenergic regulation of GP isoforms is unclear. Current studies addressed the premise that VMN ERα and/or ERβ signaling may shape differential effects of NE on VMN GPbb versus GPmm protein expression and that ER control of glycogen metabolic enzyme profiles may correlate with observed noradrenergic regulation of nNOS or GAD.

Materials and Methods

Animals

Adult female Sprague Dawley rats (240–270 g bw) were housed in groups of 2 to 3 per cage under a 14 hr light/ 10 hr dark cycle (lights on at 05.00 hr). Animals had *ad libitum* access to standard laboratory chow and water. Animals were acclimated to daily handling. All surgical and experimental protocols were conducted in accordance with National Institutes of Health guidelines for care and use of laboratory animals and approved by the University of Louisiana Monroe Institutional Animal

Care and Use Committee. On study Day 1, rats were anesthetized with ketamine/xylazine (0.1 ml/100 g bw; 90 mg ketamine:10 mg xylazine/ml; Henry Schein Inc., Melville, NY) and then bilaterally OVX and implanted with a 26-gauge double stainless-steel cannula guide (prod no. C235G-1.2/SPC; Plastics One, Inc., Roanoke, VA) aimed at the VMN (coordinates: 2.85 mm posterior to *bregma*, 0.6 mm lateral to midline, 9.0 mm below skull surface; Alhamami et al., 2018) using a computerized Neurostar GmbH Drill & Microinjection Robot (Tubingen, Germany). After surgery, rats were treated by intramuscular injection of enrofloxacin (Enroflox 2.27%, 10 mg/kg bw) and subcutaneous (*sc*) injection of ketoprofen (3 mg/kg bw) and then transferred to individual cages. On Day 7, animals were implanted with a *sc* silastic capsule (10 mm/100 g bw, 0.062 in. *i.d*, 0.125 in. *o.d.*) containing 30 µg estradiol benzoate/ml safflower oil, under isoflurane anesthesia. This steroid replacement regimen yields approximate plasma estradiol concentrations of 22 pg/ml (Briski et al., 2001), which replicate circulating hormone levels characteristic of metestrus in 4-day estrous cycles in ovary-intact female rats (Butcher et al., 1974).

Experimental Design

At 08.45 hr on Day 10, rats were pretreated by bilateral intra-VMN infusion, over a 2-min period, with the vehicle dimethyl sulfoxide (Veh, 0.5 µl; Groups 1 and 2, $n = 6$ per group); the ERα antagonist MPP (2.78 ng/0.5 µl; Tocris/Bio-Techne Corp., Minneapolis, MN; Kim and Frick, 2017; Groups 3 and 4, $n = 6$ per group); or the ERβ antagonist PHTPP (2.12 ng/0.5 µl; Tocris; Kim and Frick, 2017; Groups 5 and 6, $n = 6$ per group), using a double 33-gauge internal injection cannula (C235I-1.2/SPC; Plastics One; 0.6 mm projection beyond guide) and a Genie Touch syringe pump (Lucca Technologies, Harwinton, CT). At 9.00 hr on Day 10, dimethyl sulfoxide (V; Groups 1, 3, and 5) or NE (0.5 µg/0.5 µl; McCarren et al., 2014; Mahmood et al., 2019; Sigma Aldrich, St. Louis, MO; Groups 2, 4, and 6) was administered to the VMN over a 2-min interval. Animals were sacrificed at 11:00 hr on Day 10 for brain tissue and trunk blood collection. Dissected brains were immediately snap-frozen in liquid nitrogen-cooled isopentane and stored at –80°C. Accuracy of cannula targeting of the VMN was verified by visual examination of consecutive frozen tissue sections cut through that structure for micropunch or laser dissection.

Western Blot Analysis of Micropunch-Dissected VMN Tissue

Each forebrain was cut into alternating series of 100-µm- or 10-µm-thick frozen sections over the length of the

VMN, over repeating distances of 200 µm (2×100 µm sections) and 100 µm (10×10-µm-thick sections), respectively. VMN tissue was micropunch-dissected from 100-µm sections using 0.50-mm diameter hollow kneedles (Stoelting, Inc., Wood Dale, IL) and collected into lysis buffer (2.0% sodium dodecyl sulfate [SDS], 0.05 M dithiothreitol, 10.0% glycerol, 1.0 mM EDTA, 60 mM Tris-HCl, pH 7.2) for heat denaturation, as described (Mandal et al., 2017; Alhamami et al., 2018). For each protein of interest, three separate tissue aliquot pools were created for each treatment group prior to separation in BioRad TGX 10% stain-free gels (prod. no. 161-0183, Bio-Rad Laboratories Inc., Hercules, CA; Shakya et al., 2018). After electrophoresis, gels were activated for 1 min by UV light in a BioRad ChemiDoc TM Touch Imaging System. Proteins were transblotted to 0.45-µm polyvinylidene fluoride (PVDF)-Plus membranes (prod. no. PV4HY00010; Osmonics, Gloucester, MA).Membranes were blocked for 2 hr with Tris-buffered saline (TBS), pH 7.4, supplemented with 0.1% Tween-20 (CAS No. 9005-64-5; VWR) and 2% bovine serum albumin (ProLiant Biologicals, Boone, IA) before incubation at 4°C with primary antisera for 24 to 48 hr. Membrane buffer washes and antibody incubations were carried out by Freedom Rocker^{TM} Blotbot$^{®}$ automation (Next Advance, Inc., Troy, NY). Proteins of interest were probed with primary antisera raised in rabbit against nNOS (prod. no. NBP1-39681, 1:2,000; Novus Biologicals, Littleton, CO), GAD (prod. no. ABN904, 1:5,000; EMD Millipore, Burlington, MA), GS (prod. no. 3893S, 1:2,000; Cell Signaling Technology; Danvers, MA), GPmm (prod. no NBP2-16689, 1:2,000; Novus Biologicals), or GPbb (prod. no. NBP1-32799, 1:2,000; Novus Biologicals). Membranes were next incubated for 1 hr with a horseradish peroxidase-labeled goat antirabbit antiserum (prod. no. NEF812001EA, PerkinElmer, Boston, MA; 1:5,000). After exposure to SuperSignal West Femto maximum-sensitivity chemiluminescent substrate (prod. no. 34096, ThermoFisherScientific), protein band optical density (O.D.) signals were detected and quantified in a Bio-Rad ChemiDoc MP Imaging System equipped with Image Lab^{TM} 6.0.0, build 25, 2017, and normalized to total in-lane protein. Precision plus protein molecular weight dual color standards (prod. no. 161-0374, Bio-Rad Laboratories Inc.) were included in each Western blot analysis.

VMN Glucoregulatory Neuron Laser-Catapult Microdissection and Western Blotting

Frozen sections (10 µm thick) obtained at regular intervals over the VMN were mounted on polyethylene naphthalate membrane-coated slides (Carl Zeiss Microscopy, GmbH), and processed by avidin-biotin peroxidase immunocytochemistry to identify GAD$_{65/57}$- and

nNOS-ir neurons, as described (Ibrahim et al., 2019). Briefly, after acetone fixation (5 min) and blocking with 1.5% normal goat serum (prod. no. S-2000, Vector Laboratories, Burlingame, CA) in TBS containing 0.05% Triton X-100 (1 hr), tissues were incubated for 36 to 48 hr at 4°C with rabbit primary antibodies raised against $GAD_{65/67}$ (prod. no. ABN904, 1:1,000; MilliporeSigma, Burlington, MA) or nNOS (prod. no. NBP1-39681, 1:1,000; Novus Biologicals), followed by treatment (1 hr) with a horseradish peroxidase-labeled goat antirabbit secondary antiserum (prod. no. PI-1000, 1:1000; Vector Laboratories). Labeled neurons were visualized using Vector ImmPACT 3,3′-diaminobenzidine peroxidase substrate kit reagents (prod. no. SK-4105; Vector Laboratories). GAD- and nNOS-ir neurons were harvested from sections using a Zeiss P.A.L.M. UV-A microlaser IV and collected into lysis buffer, as described above. In previous studies, Western blot analyses were performed on nNOS- and $GAD_{65/67}$-ir cell lysates to verify nNOS or $GAD_{65/67}$ protein expression, respectively, using antibodies described earlier (Uddin et al., 2019). For each treatment group, individual target proteins were probed in separate triplicate pools of $n = 50$ GAD or nNOS neurons using BioRad TGX 10% stain-free gels (prod. no. 161-0183, Bio-Rad Laboratories Inc., Hercules, CA; Shakya et al., 2018). After electrophoresis, gels were UV light-activated (1 min) in a Bio-Rad ChemiDoc TM Touch Imaging System before transblotting (30 V, overnight at 4°C; Towbin buffer) to 0.45-μm PVDF-Plus membranes. After blocking with TBS, pH 7.4, containing 0.1% Tween-20 and 2% bovine serum albumin, membranes were incubated overnight (4°C) with primary antisera raised in rabbit against $α_1AR$ (1:2,000; prod. no. NB100-78585; Novus Biologicals) or $α_2AR$ (1:2,000; prod. no. NBP2-22452; Novus Biologicals), or in goat against $β_1AR$ (1:2,000; prod. no. NB600-978; Novus Biologicals) or MCT2 (1:2,000; prod. no. AB3542; EMD Millipore, Billerica, AM). Membranes were exposed to peroxidase-conjugated goat anti-rabbit (1:5,000; NEF812001EA; PerkinElmer, Billerica, MA) or rabbit anti-goat (1:5,000; prod. no. AP106P; EMD Millipore, Billerica, MA) secondary antibodies prior to incubation with SuperSignal West Femto chemiluminescent substrate (34096; ThermoFisherScientific). Membrane buffer washes and antibody incubations were carried out by Freedom Rocker™ Blotlbot® automation. Protein O.D.s generated from chemiluminescent substrate were detected and processed by Bio-Rad Stain-Free Imaging Technology, as described earlier. Bio-Rad precision plus protein molecular weight dual color standards (prod. no. 161-0374) were included in each Western blot analysis.

Glucose and Counter-Regulatory Hormone Measurements

Blood glucose levels were determined using an ACCU-CHECK Aviva plus glucometer (Roche Diagnostic Corporation, Indianapolis, IN; Kale et al., 2006). Plasma free fatty acid (FFA) concentrations were measured with Free Fatty Acid Quantitation Kit reagents (MAK044; Sigma Aldrich, St. Louis, MO; Briski et al., 2017). Plasma corticosterone (ADI-900-097; Enzo Life Sciences, Inc., Farmingdale, NY) and glucagon (EZGLU-30K, EMD Millipore, Billerica, MA) concentrations were determined using commercial ELISA kit reagents, as described (Alhamami et al., 2018).

Statistical Analyses

Mean normalized tissue protein O.D., glucose, glucagon, corticosterone, and FFA data were evaluated between treatment groups by two-way analysis of variance for ER, with ER pretreatment and NE treatment as factors, and Student–Newman–Keuls post hoc test. Statistical analyses were performed using Graph pad prism 5.0 and IBM SPSS Statistics 22.0. Differences of $p < .05$ were considered significant.

Results

Figure 1 depicts combinatory VMN nitrergic and GABAergic neuron immunocytochemical labeling and laser-catapult microdissection. Individual nerve cells in VMH tissue sections were identified by $GAD_{65/67}$- (Panel 1A) or nNOS- (Panel 1B)-immunoreactivity prior to laser-catapult harvesting (left-hand column); representative labeled neurons are indicated by blue arrows. Middle and right-hand columns illustrate actions, including sequential positioning of a continuous laser cut (shown in green in Panels 1B and 2B) surrounding a distinctive neuron, that result in removal of single cells without destruction of surrounding tissue and minimal inclusion of adjacent tissue (Panels 1C and 2C). Representative immunoblots presented in Panels 1D and 2D indicate that $GAD_{65/67}$ or nNOS protein is expressed in cells harvested by combinatory immunocytochemistry/laser-catapult microdissection.

Effects of intra-VMN NE administration on VMN nNOS and GAD protein expression were evaluated after ER antagonist or vehicle pretreatment (Figure 2). Data presented in Panel 2A show that MPP or PHTPP significantly reduced VMN nNOS profiles compared with controls (MPP/Veh and PHTPP/Veh vs. Veh/Veh). NE decreased tissue nNOS levels (Veh/NE vs. Veh/Veh); neither ER antagonist altered this response. As shown in Panel 2B, VMN GAD protein expression was unaffected by either MPP or PHTPP. Yet, NE
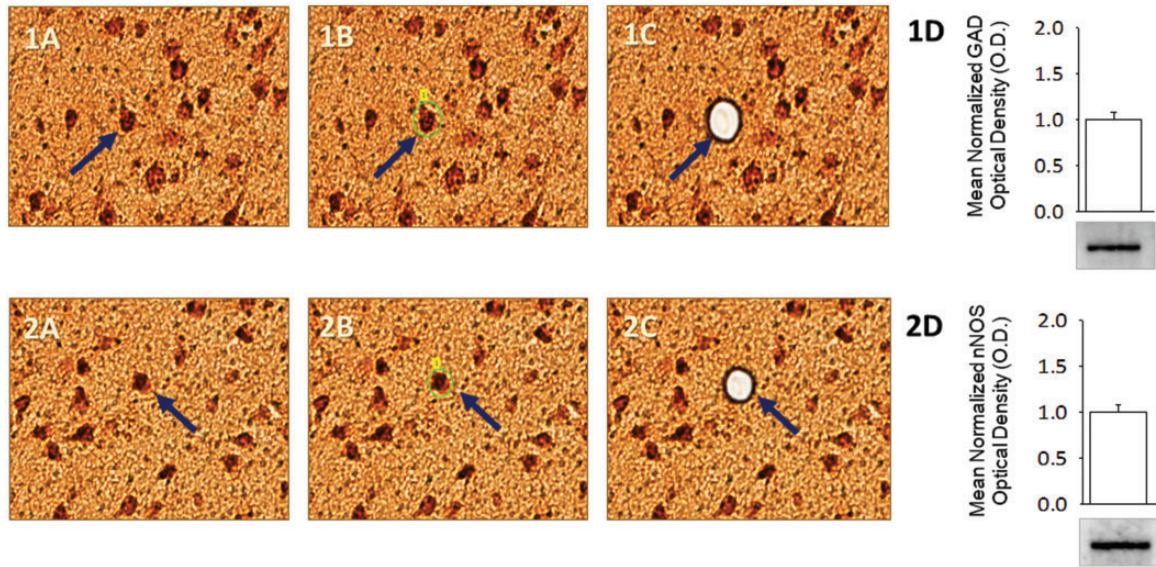
Figure 1. Laser-Catapult Microdissection of Immunolabeled ventromedial hypothalamic nucleus (VMN) GABA or Nitrergic Neurons: Western Blot Confirmation of Accuracy of Immunocytochemical Identification of Neurotransmitter Phenotype. VMN neurons were identified *in situ* for glutamate decarboxylase$_{65/67}$ (GAD$_{65/67}$)- (top row, Panel 1A) or neuronal nitric oxide (nNOS)-immunoreactivity (-ir) (bottom row, Panel 2A); representative GAD$_{65/67}$- or nNOS-ir-positive neurons are indicated by blue arrows. Areas shown in Panels 1A and 2A were rephotographed after positioning of a continuous laser track (depicted in green) around a single GAD$_{65/67}$-ir (Panel 1B, blue arrow) or nNOS-ir neuron (Panel 2B, blue arrow) and subsequent ejection of the encircled cell by laser pulse (Panels 1C and 2C). Note that this microdissection technique causes negligible destruction of surrounding tissue and minimal inclusion of adjacent tissue. Western blot analysis of triplicate cell lysate pools produced from immunolabeled GAD$_{65/67}$ (Panel 1D) or nNOS (Panel 2D) neurons from Veh/Veh animals showed that these proteins are expressed in VMN neuron samples obtained by combinatory immunocytochemistry/laser-catapult microdissection.
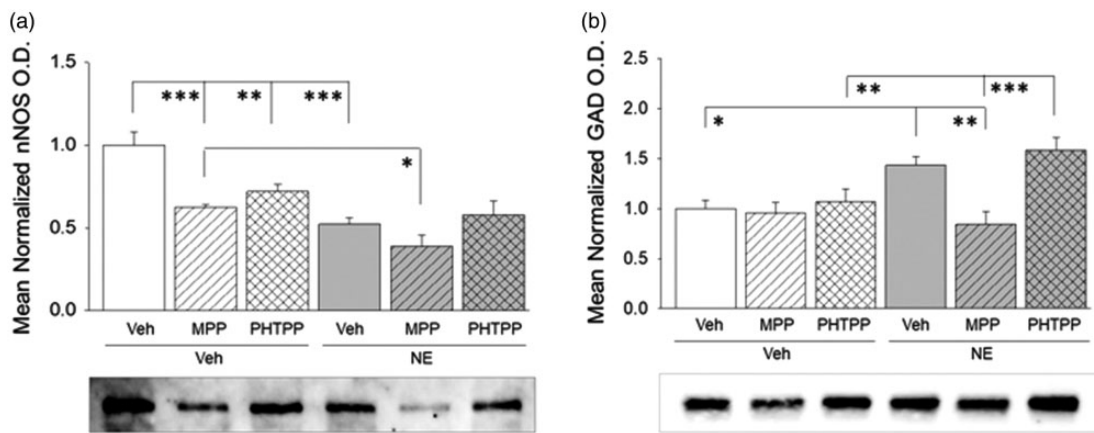
Figure 2. Effects of ERα and ERβ Antagonists on NE Regulation of VMN GAD and nNOS Protein Expression. Micropunch-dissected VMN tissue was obtained from groups of ovariectomized, estradiol-replaced female rats pretreated by intra-VMN delivery of MPP, PHTPP, or vehicle (Veh) prior to NE administration for Western blot analysis of neuronal nitric oxide synthase (nNOS)—Panel 2A, $F(5, 12) = 12.67$, $p < .0001$—or glutamate decarboxylase$_{65/67}$ (GAD)—Panel 2B, $F(5, 12) = 7.13$, $p = .0003$—protein expression. Data depict mean normalized protein optical density (O.D.) values $\pm$ *SEM* for groups of rats ($n = 6$ per group) infused with Veh (white bars) or NE (gray bars) after delivery of Veh (solid bars), MPP (diagonal-striped bars), or PHTPP (cross-hatched bars) administration. $*p < .05$; $**p < .01$; $***p < .001$. MPP = 1,3-*Bis*(4-hydroxyphenyl)-4-methyl-5-[4-(2-piperidinylethoxy)phenol]-1*H*-pyrazole dihydrochloride; PHTPP = 4-[2-phenyl-5,7-*bis*(trifluoromethyl)pyrazolo[1,5-*a*]pyrimidin-3-yl]phenol; NE = norepinephrine.
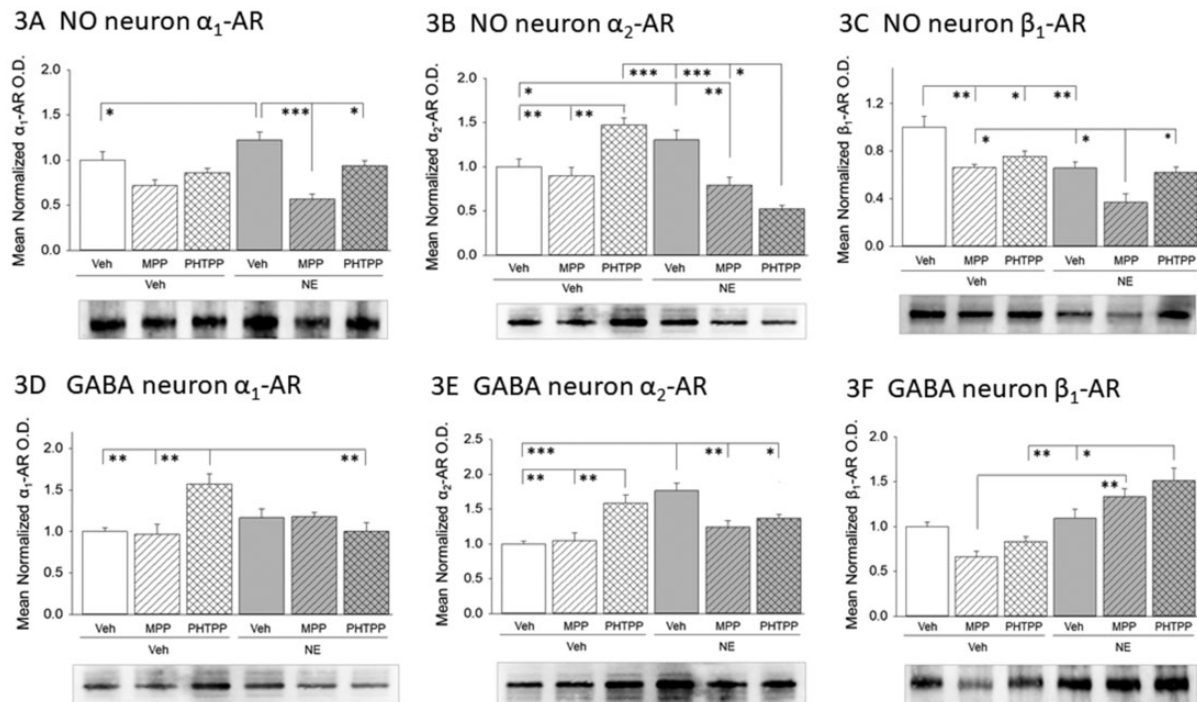
Figure 3. Effects of MPP Versus PHTPP on NE Regulation of VMN Nitrergic and GABA Neuron Adrenergic Receptor Protein Expression. Pooled lysates of laser-microdissected VMN nNOS- or GAD-immunopositive neurons from groups of female rats pretreated with V versus ERα or -β antagonist prior to intra-VMN V or NE infusion were analyzed by Western blot for alpha$_1$- (α_1-), alpha$_2$- (α_2-), or beta$_1$- (β_1-) AR protein expression. Nitrergic neuron α_1-, $F(5, 12) = 10.51$, $p = .0005$; α_2-, $F(5, 12) = 16.50$, $p < .0001$; and β_1-, $F(5, 12) = 11.72$, $p = .0003$ protein profiles are depicted in Panels 3A to C; GABAergic neuron α_1-, $F(5, 12) = 5.52$, $p = .007$; α_2-, $F(5, 12) = 10.47$, $p < .0001$; and β_1-, $F(5, 12) = 12.21$, $p = .0002$ protein profiles are presented in Panels 3D to F. Data show mean normalized protein O.D. measures ± SEM for the following treatment groups: Veh/Veh (solid white bars, $n = 6$), MPP/Veh (diagonal-striped white bars, $n = 6$), PHTPP/Veh (cross-hatched white bars, $n = 6$), Veh/NE (solid gray bars, $n = 6$), MPP/NE (diagonal-striped gray bars, $n = 6$), and PHTPP/NE (cross-hatched gray bars, $n = 6$). *$p < .05$; **$p < .01$; ***$p < .001$. α_1-AR = alpha$_1$ adrenergic receptor; α_2-AR = alpha$_2$ adrenergic receptor; β_1-AR = beta$_1$ adrenergic receptor; MPP = 1,3-Bis(4-hydroxyphenyl)-4-methyl-5-[4-(2-piperidinylethoxy)phenol]-1H-pyrazole dihydrochloride; PHTPP = 4-[2-phenyl-5,7-bis(trifluoromethyl)pyrazolo[1,5-a]pyrimidin-3-yl]phenol; NE = norepinephrine.

augmentation of GAD profiles was significantly attenuated by MPP pretreatment (MPP/NE vs. Veh/NE).

Effects of VMN ER antagonism on noradrenergic regulation of nitrergic and GABAergic nerve cell α_1-, α_2-, and β_1-AR protein expression are presented in Figure 3. Data in Panel 3A show that neither MPP nor PHTPP modified nitrergic α_1-AR protein content. NO nerve cell α_1-AR levels were elevated in Veh/NE versus Veh/Veh treatment groups, and MPP pretreatment reversed this stimulatory response to NE. Nitrergic cell α_2-AR profiles were elevated by PHTPP but not MPP. Noradrenergic augmentation of α_2-AR expression in these neurons was reversed by MPP or PHTPP preexposure (Panel 3B). NO nerve cell β_1-AR protein expression was suppressed by either MPP or PHTPP; NE-associated reductions in this were exacerbated by MPP pretreatment (Panel 3C). Data in Panel 3D show that GABA neuron α_1-AR levels were amplified by PHTPP but were refractory to NE. GABA α_2-AR expression was elevated by PHTPP or NE. Noradrenergic stimulation of this profile

was averted by MPP or PHTPP pretreatment. As shown in Panel 3F, GABA β_1-AR expression in Veh- or NE-infused rats was unaffected by either antagonist.

Effects of NE on MCT2 protein expression in VMN glucoregulatory neurons were evaluated after ER antagonist or vehicle pretreatment (Figure 4). Nitrergic (Panel 4A) and GABAergic (Panel 4B) neuron MCT2 profiles were unaffected by MPP or PHTPP. While MCT2 protein levels were equivalent after V versus NE treatment, this profile was significantly decreased in NO and GABA neurons in MPP/NE versus Veh/NE treatment groups.

Intra-VMN effects of NE on GS, GPbb, and GPmm protein profiles were examined in animals pretreated with ER antagonist or vehicle (Figure 5). Data in Panel 5A indicate that GS protein expression was not altered after exposure to either ER antagonist and was inhibited by NE by ER-independent mechanisms. As shown in Panel 5B, VMN GPbb profiles were refractory to MPP and PHTPP; however, noradrenergic augmentation of GPbb expression was reversed by either MPP or
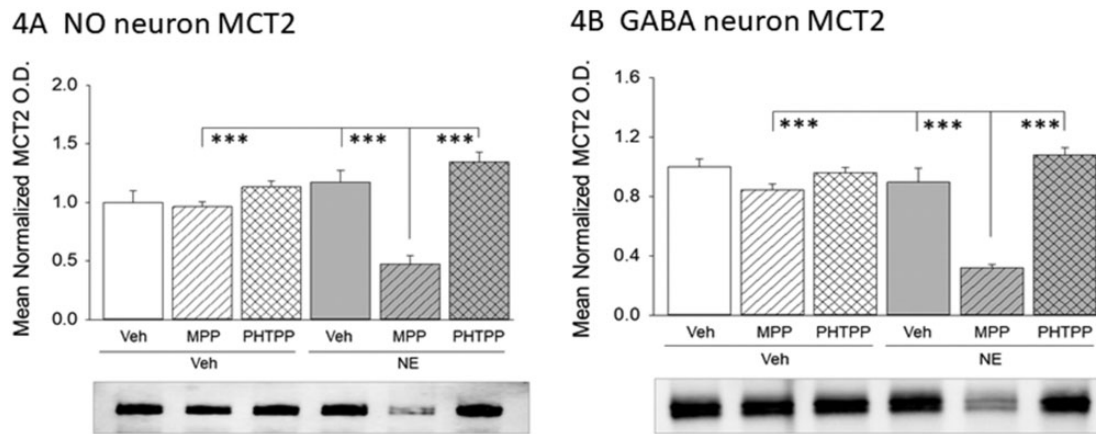
Figure 4. Effects of MPP or PHTPP on NE Regulation of VMN Nitrergic and GABAergic Neuron MCT2 Protein Expression. Pooled lysates of laser-microdissected VMN nNOS- or GAD-immunopositive neurons from groups of V- versus ER antagonist-pretreated, V- or NE-treated rats were analyzed by Western blot for MCT2. Data show mean normalized nitrergic (Panel 4A), $F_{(5, 12)} = 14.86$, $p < .0001$, and GABAergic (Panel 4B), $F_{(5, 12)} = 25.43$, $p < .0001$, nerve cell MCT2 protein O.D. measures $\pm$ SEM for Veh/Veh (solid white bars, $n = 6$), MPP/Veh (diagonal-striped white bars, $n = 6$), PHTPP/Veh (cross-hatched white bars, $n = 6$), Veh/NE (solid gray bars, $n = 6$), MPP/NE (diagonal-striped gray bars, $n = 6$), and PHTPP/NE (cross-hatched gray bars, $n = 6$) treatment groups. $*p < .05$; $**p < .01$; $***p < .001$. MPP = 1,3-Bis(4-hydroxyphenyl)-4-methyl-5-[4-(2-piperidinylethoxy)phenol]-1H-pyrazole dihydrochloride; PHTPP = 4-[2-phenyl-5,7-bis(trifluoromethyl)pyrazolo[1,5-a]pyrimidin-3-yl]phenol; NE = norepinephrine; MCT2 = monocarboxylate transporter-2.
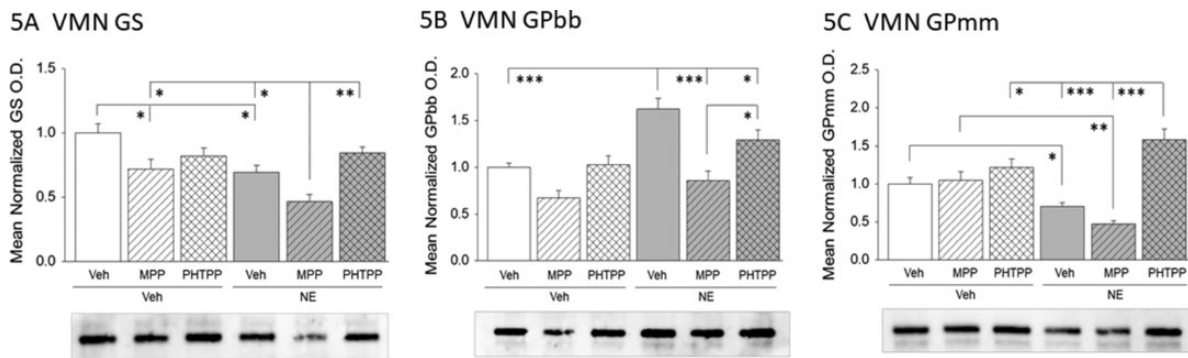
Figure 5. ERα and ERβ Involvement in Noradrenergic Regulation of VMN GS and GPbb/GPmm Protein Expression. Micropunch-dissected VMN tissue obtained from groups of female rats ($n = 6$/group) infused into the VMN with Veh or NE after Veh, MPP, or PHTPP pretreatment was analyzed by Western blot for GS (Panel 5A), $F_{(5, 12)} = 8.44$, $p = .0003$; GPbb (Panel 5B), $F_{(5, 12)} = 12.90$, $p < .0001$; or GPmm (Panel 5C), $F_{(5, 12)} = 16.49$, $p < .0001$ protein content. Data show mean normalized protein optical density (O.D.) values $\pm$ SEM. $*p < .05$; $**p < .01$; $***p < .001$. VMN = ventromedial hypothalamic nucleus; GS = glycogen synthase; GPmm = glycogen phosphorylase-muscle type; GPbb = glycogen phosphorylase-brain type; MPP = 1,3-Bis(4-hydroxyphenyl)-4-methyl-5-[4-(2-piperidinylethoxy)phenol]-1H-pyrazole dihydrochloride; PHTPP = 4-[2-phenyl-5,7-bis(trifluoromethyl)pyrazolo[1,5-a]pyrimidin-3-yl]phenol; NE = norepinephrine.

PHTPP. VMN GPmm content was also unaffected by ER antagonist administration, but NE-associated reductions in this profile were averted by PHTPP (Panel 5C).

Effects of NE on plasma glucose, counter-regulatory hormone, and FFA levels were investigated after intra-VMN ER antagonist or vehicle pretreatment (Figure 6). Panels 6A and 6B show that corresponding plasma glucose and glucagon concentrations were unaffected by MPP or PHTPP treatment alone or in combination with NE. Data in Panel 6C demonstrate that corticosterone secretion is refractory to antagonism of VMN ERα or $-\beta$ but that NE-associated elevations in hormone release were attenuated by MPP or PHTPP. Circulating FFA levels (Panel 6D) were not altered by exposure to either MPP or PHTPP alone, but noradrenergic augmentation of plasma FFA was diminished by MPP or PHTPP pretreatment.

Discussion

Current studies provide unique evidence that VMN ERα and ERβ stimulate basal NO signaling and that noradrenergic augmentation of GABA transmission involves ERα (Figure 7). Results show that these ERs exert

6A Plasma Glucose

6B Plasma Glucagon

## 6C Plasma Corticosterone

6D Plasma FFA
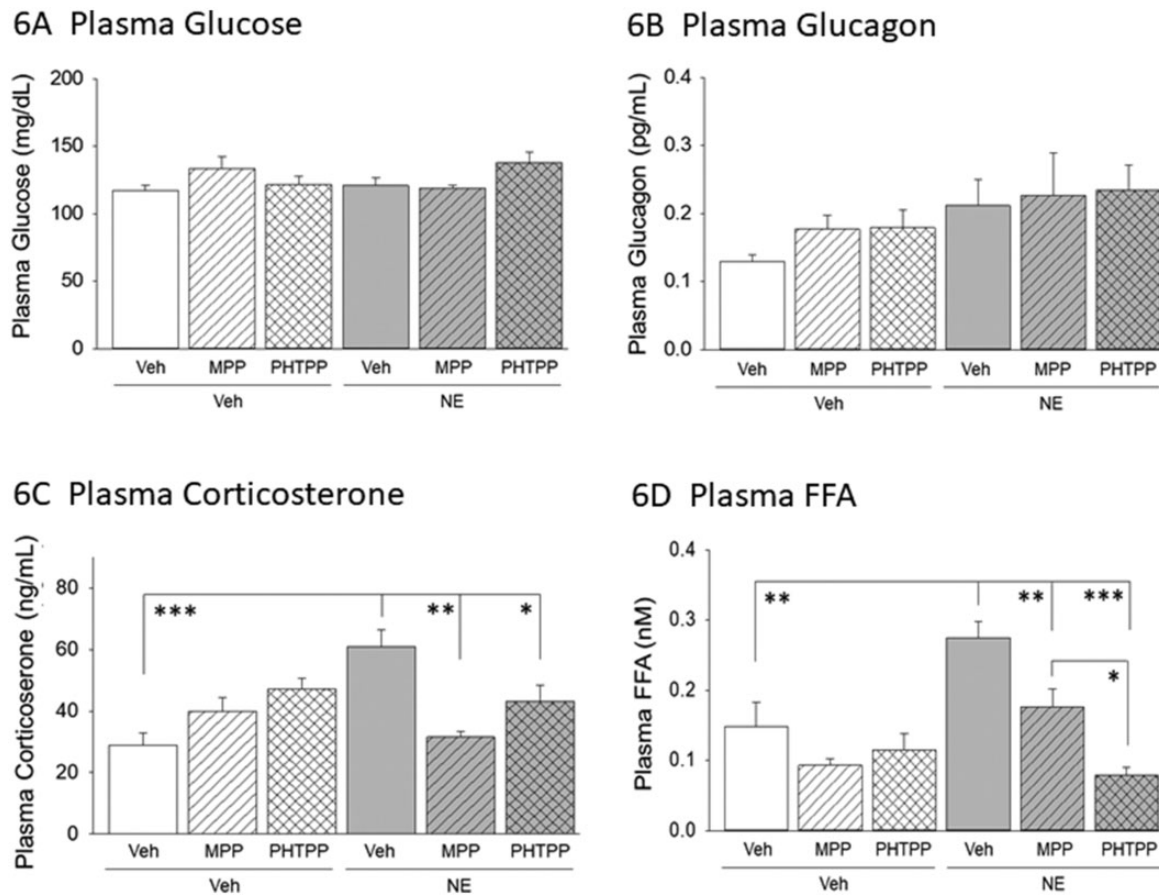
Figure 6. Effects of MPP or PHTPP Pretreatment on Effects of Intra-VMN NE Administration on Circulating Glucose, Counter-Regulatory Hormone, and FFA Levels. Data show mean plasma glucose (Panel 6A), $F_{(5, 30)} = 1.87$, $p = .13$; glucagon (Panel 6B), $F_{(5, 30)} = 1.14$, $p = .37$; corticosterone (Panel 6C), $F_{(5, 30)} = 6.38$, $p = .0009$; and FFA (Panel 6D), $F_{(5, 30)} = 11.26$, $p < .0001$ concentrations $\pm$ *SEM* for groups of Veh- or NE-infused animals that were pretreated with Veh, MPP, or PHTPP ($n = 6$/treatment group). FFA = plasma free fatty acid; MPP = 1,3-*Bis*(4-hydroxyphenyl)-4-methyl-5-[4-(2-piperidinylethoxy)phenol]-1*H*-pyrazole dihydrochloride; PHTPP = 4-[2-phenyl-5,7-*bis*(trifluoromethyl)pyrazolo[1,5-*a*]pyrimidin-3-yl]phenol; NE = norepinephrine.

disparate effects on transmitter marker and AR protein expression in NO versus GABA cells and their actions in each cell type are regulated by NE. Data indicate that estradiol and NE may also interact within the astrocyte compartment to control stimulus-specific glycogen breakdown.

Present data document ERα and −β regulation of homeostatic patterns of nNOS but not GAD protein profiles. As NO neurons contain ER proteins (Uddin et al., 2019), intrinsic ER likely mediate estradiol stimulation of nNOS expression. Results affirm prior reports that in female rats, site-specific targeting of exogenous NE to the VMN elicits concomitant down- versus upregulation of glucostimulatory (nNOS) and glucoinhibitory (GAD) signaling marker proteins, which infers that VMN neuroenergetic stability is enhanced by NE (Mahmood et al., 2019). This assumption remains unverified as methodology to support analysis of single-nerve cell ATP content is currently unavailable; thus, definitive

evidence that glucoregulatory transmitter responses to NE reflect a positive shift in energy state is yet to be attained. Data here show that noradrenergic augmentation of GAD is ERα-dependent, whereas suppression of nNOS does not require ER. Further studies are needed to determine if strength, for example, volume of NE input to the VMN governs ER variant expression, receptor interactions, and/or postreceptor signaling to thereby shape directionality or magnitude of ER control of glucoregulatory transmitter cues.

Data show that ERα and ERβ exert differential effects on basal AR protein expression in NO versus GABA neurons. NE elicited similar (α$_2$-AR) as well as divergent (α$_1$-AR; β$_1$-AR) changes in AR profiles in these two nerve cell populations. Interestingly, in the presence of exogenous NE, ERβ tonus switches from inhibitory to stimulatory regarding NO and GABA cell α$_2$-AR proteins. Likewise, ERα signaling did not regulate α$_2$-AR expression in either neuron population but was critical
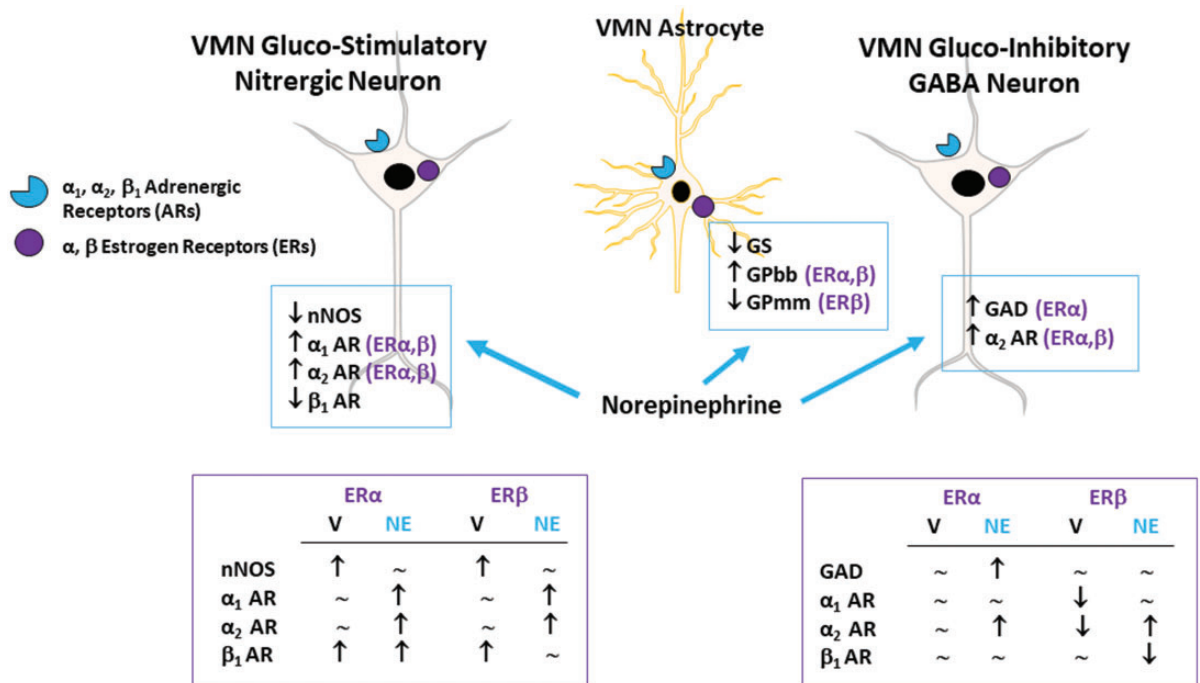
Figure 7. Model for ER and NE Interaction in Governance of VMN Glucoregulatory Transmission and Glycogen Metabolism. VMN nitrergic (left) and GABAergic (right) neurons and astrocytes (middle) express ERα and ERβ (Mahmood et al., 2019; Uddin et al., 2019) as well as α_1-AR, α_2-AR, and β_1-AR proteins (Ibrahim et al., 2019; Uddin et al., 2019). For each nerve cell type, effects of intra-VMN NE administration on transmitter marker and AR proteins are outlined in an accompanying blue box; NE effects on the astrocyte glycogen metabolic enzyme proteins GS and GP variants GPbb and GPmm are listed also. For nitrergic and GABA neurons, purple boxes depict ERα and ERβ regulation of transmitter marker and AR proteins in the absence versus presence of NE. Arrows depict direction of ER impact; absence of ER effect is indicated by horizontal dash. VMN = ventromedial hypothalamic nucleus; nNOS = neuronal nitric oxide synthase; GS = glycogen synthase; GPmm = glycogen phosphorylase-muscle type; GPbb = glycogen phosphorylase-brain type; GAD = glutamate decarboxylase$_{65/67}$; GABA = γ-aminobutyric acid; NE = norepinephrine.

for noradrenergic upregulation of this protein profile in nitrergic and GABAergic cells. As this neutral/negative-to-positive shift in ERα and ERβ influence on α_2-AR expression requires NE, a plausible interpretation is that during homeostatic patterns of noradrenergic signaling, estradiol may act on these ER to diminish VMN NO and GABA nerve cell sensitivity to NE via α_2-AR. There is an obvious need to elucidate the molecular mechanisms that underlie ER and NE interaction in the regulation of these protein profiles. It would be informative to learn if NE primes nitrergic and GABAergic neuron receptivity to catecholaminergic input via regulation of ER expression and signaling.

VMN NO and GABA nerve cell MCT2 protein profiles were refractory to MPP or PHTPP treatment, which argues against ERα or $-\beta$ involvement in regulation of lactate uptake into these nerve cell types. While MCT2 levels unaffected by NE, ERα signaling was required to maintain this protein profile after noradrenergic stimulation in each neuron population. It is presumed that NE input to the VMN promotes ERα participation in MCT2 expression in both glucoregulatory cell populations. As noradrenergic stimulation of local glycogen breakdown is

also ERα-dependent, concerted ERα action on astrocyte and metabolic neurons may result in optimized transfer of glycogen-derived energy fuel between these cell compartments. As current studies focused on a singular time point after NE delivery to VMN for protein analyses, the possibility cannot be overlooked that MCT2 expression in NO and/or GABA neurons may vary between NE versus Veh groups at a timing before or after +2 hr.

Differential ERα and ERβ antagonist effects on nitrergic versus GABAergic transmitter marker and α_1-/β_1-AR protein expression may reflect, in part, variances in absolute numbers and/or ratio of ERα and ERβ protein expression between the two neuron populations. There may also be disparate regulation of post-ERα and/or ERβ signaling, particularly if there are differences in partitioning of ER between cytosol versus plasma membrane in these nerve cell types. Furthermore, ER regulatory effects could be subject to discrepant modulation by other hormonal or transmitters signals to these neurons.

Current studies provide unique evidence for divergent effects of NE on AMP-sensitive GPbb (upregulated) versus NE-sensitive GPmm (downregulated) protein expression in the female rat VMN. These results concur

with recent evidence in the male rat that alpha-cyano-4-hydroxycinnamic acid-induced hindbrain lactoprivic signaling, which is mediated by A2 noradrenergic neurons (Shrestha et al., 2014), amplifies VMN GPbb protein content while at the same time diminishing tissue GPmm levels (Briski and Mandal, 2019). Those findings suggest that hindbrain metabolic deficit-driven patterns of VMN NE activity may facilitate VMN glycogenolysis by GPbb activation by local indicators of energy insufficiency, for example, AMP. Data here show that classical ER signaling has no likely impact on VMN GP isoform expression during homeostasis but that ERα and ERβ are required for NE augmentation of GPbb or noradrenergic suppression of GPmm, respectively, inferring that each ER is recruited by NE to regulate a distinctive GP variant.

Evidence here and elsewhere (Briski and Mandal, 2019) for coincident noradrenergic regulation of VMN GAD and GP isoform protein profiles raises the possibility that glycogen metabolism status may influence GABA transmission. It can be speculated that VMN GABA neurons may interpret attenuated NE-driven glycogen breakdown due to downregulated GPmm protein as an indicator of increased energy reserve mass. At the same time, NE-associated amplification of GPbb profiles, in the absence of local metabolic imbalance, may likely further diminish glycogen mobilization and enhance the glycogen reserve, which in turn may reinforce communication of a gain in astrocyte energy surplus to those neurons. Evidence for parallel ERα involvement in noradrenergic upregulation of GPbb and GAD profiles implies that a potential cause-and-effect relationship between these protein responses may exist. As current studies did not measure VMN tissue glycogen, it remains to be proven whether net glycogen mass is expanded by the current NE treatment paradigm, and if so, whether glycogen volume or turnover is a crucial variable that is monitored by GABA neurons.

Present data show that +2 hr after intra-VMN NE administration, plasma glucose levels were measurable within the normal range, while circulating corticosterone and FFA concentrations were elevated. Previous observations of NE-associated mild hypoglycemia and unmodified FFA values at 1 hr posttreatment indicate that these specific responses adhere to distinctive temporal patterns, whereas hypercorticosteronemia is a uniform reaction, at least up to 2 hr posttreatment (Mahmood et al., 2019). Earlier studies showed that pharmacological inhibition of VMN GP activity by 1,4-dideoxy-1,4-imino-D-arabinitol did not alter euglycemic patterns of corticosterone secretion but prevented hypoglycemic hypercorticosteronemia (Alhamami et al., 2018). Those results support the prospect that noradrenergic suppression of VMN GPmm expression may not be a factor in elevated corticosterone output observed here in NE-treated animals. Additional effort will be required to clarify whether noradrenergic stimulation of corticosterone involves, in part, direct action on VMN GABA and/or NO neurons.

While current data provide new insight concerning classical ER involvement in regulation of protein markers of VMN glycogen metabolism and metabolic transmitter release, it is plausible that some or all estradiol modulatory effects described here may involve GPER signaling. Observations that ERα and ERβ stimulate VMN nitrergic nerve cell GPER profiles whereas ERα signaling inhibits GPER expression in GABAergic neurons during hypoglycemia (Uddin et al., 2019) support speculation that distinctive actions of each ER, alone or in the presence of NE, on current endpoints may require adjustments in GPER signaling. However, further studies are needed to address this premise.

In summary, current research addressed the premise that VMN ERα and/or -β control basal and/or noradrenergic stimulation-driven patterns of local nitrergic and GABAergic transmission. Results document unique ERα and ERβ actions on metabolic transmitter and AR protein expression in VMN nitrergic versus GABAergic neurons. ER effects varied in the presence versus absence of NE, indicating that both neuron types are substrates for estradiol and noradrenergic regulatory interaction. NE-dependent ER control of VMN GP variant expression implies that these signals also act on astrocytes to direct physiological stimulus-specific control of glycogen metabolism, which may in turn influence GABA transmission. Further studies are needed to elucidate the molecular mechanisms by which NE controls the direction of ER regulation, for example, stimulation versus inhibition of VMN glucoregulatory neuron receptivity to noradrenergic signaling.

Declaration of Conflicting Interests

Funding

ORCID iD

Karen P. Briski ⬤ https://orcid.org/0000-0002-7648-1395

References

Alhamami, H. N., Alshamrani, A., & Briski, K. P. (2018). Effects of the glycogen phosphorylase inhibitor 1,4-dideoxy-1,4-imino-D-arabinitol on ventromedial hypothalamic nucleus 5'-adenosine monophosphate-activated protein kinase activity and metabolic neurotransmitter biosynthetic enzyme protein expression in eu- versus hypoglycemic male rats. *Physiol Rep*, *103*, 236–249.

Ashford, M. L. J., Boden, P. R., & Treherne, J. M. (1990). Glucose-induced excitation of hypothalamic neurons is mediated by ATP-sensitive K+ channels. *Pfugers Arch*, *415*, 479–483.

Briski, K. P., Alenazi, F. S. H, Shakya, M., & Sylvester, P. W. (2017). Estradiol regulates hindbrain A2 noradrenergic neuron adenosine 5'-monophosphate-activated protein kinase (AMPK) activation, upstream kinase/phosphatase protein expression, and receptivity to hormone and fuel reporters of short-term food deprivation in the ovariectomized female rat. *J Neurosci Res*, *95*, 1427–1437.

Briski, K. P., & Mandal, S. K. (2019). Hindbrain lactoprivic regulation of hypothalamic neuron transactivation and gluco-regulatory neurotransmitter expression: Impact of antecedent insulin-induced hypoglycemia. *Neuropeptides*, *77*, 101962. 10.1016/j.npep.2019.101962

Briski, K. P., Marshall, E. S., & Sylvester, P. W. (2001). Effects of estradiol on glucoprivic transactivation of catecholaminergic neurons in the female rat caudal brainstem. *Neuroendocrinology*, *73*, 369–377.

Briski, K. P., & Nedungadi, T. P. (2009). Adaptation of feeding and counter-regulatory hormone responses to intermediate insulin-induced hypoglycaemia in the ovariectomised female rat: Effects of oestradiol. *J Neuroendocrinol*, *21*, 578–585.

Butcher, R. L., Collins, W. E., & Fugo, N. W. (1974). Plasma concentrations of LH, FSH, progesterone, and estradiol-17beta throughout the 4-day estrous cycle of the rat. *Endocrinology*, *94*, 1704–1708.

Chan, O., Zhu, W., Ding, Y., McCrimmon, R. J., & Sherwin, R. S. (2006). Blockade of GABA(A) receptors in the ventromedial hypothalamus further stimulates glucagon and sympathoadrenal but not the hypothalamo-pituitary-adrenal response to hypoglycemia. *Diabetes*, *55*, 1080–1087.

Donovan, C. M., & Watts, A. G. (2014). Peripheral and central glucose sensing in hypoglycemic detection. *Physiology*, *29*, 314–324.

Fioramonti, X., Marsollier, N., Song, Z., Fakira, K. A., Patel, R. M., Brown, S., Duparc, T., Pica-Mendez, A., Sanders, N. M., Knauf, C., Valet, P., McCrimmon, R. J., Beuve, A., Magnan, C., & Routh, V. H. (2010). Ventromedial hypothalamic nitric oxide production is necessary for hypoglycemia detection and counterregulation. *Diabetes*, *59*, 519–528.

Goodman, R. L. (1978). A quantitative analysis of the physiological role of estradiol and progesterone in the control of tonic and surge secretion of luteinizing hormone in the rat. *Endocrinology*, *102*, 142–150.

Ibrahim, M. M. H., Alhamami, H. N., & Briski, K. P. (2019). Norepinephrine regulation of ventromedial hypothalamic nucleus metabolic transmitter biomarker and astrocyte enzyme and receptor expression: Role of 5'-AMP-activated protein kinase. *Brain Res*, *1711*, 48–57.

Kale, A.Y., Paranjape, S.A., & Briski, K.P. (2006). I.c.v. administration of the nonsteroid glucocorticoid receptor antagonist, CP-472555, prevents exacerbated hypoglycemia during repeated insulin administration. *Neuroscience*, *140*, 555–565.

Kim, J., & Frick, K. M. (2017). Distinct effects of estrogen receptor antagonism on object recognition and spatial memory consolidation in ovariectomized mice. *Psychoneuroendocrinology*, *85*, 110–114.

Mahmood, A. S. M. H., Bheemanapally, K., Mandal, S. K., Ibrahim, M. M. H., & Briski, K. P. (2019). Norepinephrine control of ventromedial hypothalamic nucleus glucoregulatory neurotransmitter expression in the female rat: Role monocarboxylate transporter function. *Mol Cell Neurosci*, *95*, 51–58.

Mahmood, A. S. M. H., Uddin, M. M., Mandal, S. K., Ibrahim, M. M. H., Alhamami, H. N., & Briski, K. P. (2018). Sex differences in forebrain estrogen receptor regulation of hypoglycemic patterns of counter-regulatory hormone secretion and ventromedial hypothalamic nucleus gluco-regulatory neurotransmitter and astrocyte glycogen metabolic enzyme expression. *Neuropeptides*, *72*, 65–74.

Mandal, S. K., Shrestha, P. K., Alenazi, F. S. H., Shakya, M., Alhamami, H. N., & Briski, K. P. (2017). Role of hindbrain adenosine 5'-monophosphate-activated protein kinase (AMPK) in hypothalamic AMPK and metabolic neuropeptide adaptation to recurring insulin-induced hypoglycemia in the male rat. *Neuropeptides*, *66*, 25–35.

McCarren, H. S., Chalifax, M. R., Han, B., Moore, J. T., Meng, Q. C., Baron-Hionis, N., Sedigh-Sarvestani, M., Contreras, D., Beck, S. G., & Kelz, M. B. (2014). α2-Adrenergic stimulation of the ventrolateral preoptic nucleus destabilizes the anesthetic state. *J Neurosci*, *34*, 16385–16396.

Müller, M. S., Pedersen, S. E., Walls, A. B., Waagepetersen, H. S., & Bak, L. K. (2015). Isoform-selective regulation of glycogen phosphorylase by energy deprivation and phosphorylation in astrocytes. *Glia*, *63*, 154–162.

Nadeau, O. W., Fontes, J. D., & Carlson, G. M. (2018). The regulation of glycogenolysis in the brain. *J Biol Chem*, *293*, 7099–7109.

Nedungadi, T. P., & Briski, K. P. (2012). Site-specific effects of intracranial estradiol administration on recurrent insulin-induced hypoglycemia in ovariectomized female rats. *Neuroendocrinology*, *96*, 311–323.

Nedungadi, T. P., Goleman, W. L., Paranjape, S. A., Kale, A. Y., & Briski, K. P. (2006). Effects of estradiol on glycemic and CNS neuronal activational responses to recurrent insulin-induced hypoglycemia in the ovariectomized female rat. *Neuroendocrinology*, *84*, 235–243.

Oomura, Y., Ono, H., Ooyama, H., & Wayner, M. J. (1969). Glucose and osmosensitive neurons of the rat hypothalamus. *Nature*, *222*, 282–284.

Routh, V. H., Hao, L., Santiago, A. M., Sheng, Z., & Zhou, C. (2014). Hypothalamic glucose sensing: Making ends meet. *Front Syst Neurosci*, *8*, 236. 10.3389/fnsys.2014.00236

Shakya, M., Shrestha, P. K., & Briski, K. P. (2018). Hindbrain 5'-adenosine monophosphate-activated protein kinase mediates short-term food deprivation inhibition of the

gonadotropin-releasing hormone-luteinizing hormone axis: Role of nitric oxide. *Neuroscience, 383*, 46–59.

Shrestha, P. K., Tamrakar, P., Ibrahim, B. A., & Briski, K. P. (2014). Hindbrain medulla catecholamine cell group involvement in lactate-sensitive hypoglycemia-associated patterns of hypothalamic norepinephrine and epinephrine activity. *Neuroscience, 278*, 20–30.

Silver, I. A., & Erecińska, M. (1998). Glucose-induced intracellular ion changes in sugar-sensitive hypothalamic neurons. *J Neurophysiol, 79*, 1733–1745.

Stobart, J. L., & Anderson, C. M. (2013). Multifunctional role of astrocytes as gatekeepers of neuronal energy supply. *Cell Neurosci, 7*, 1–21.

Uddin, M. M., Mahmood, A. S. M. H., Ibrahim, M. M. H., & Briski, K. P. (2019). Sex dimorphic estrogen receptor regulation of ventromedial hypothalamic nucleus glucoregulatory neuron adrenergic receptor expression in hypoglycemic male and female rats. *Brain Res, 1720*, 146311. 10.1016/j.brainres.2019.146311

Watts, A. G., & Donovan, C. M. (2010). Sweet talk in the brain: Glucosensing, neural networks, and hypoglycemic counterregulation. *Front Neuroendocrinol, 31*, 32–43.